

## Mid-infrared plasmon regulation based on graphene nanoribbons

HAN Jing, GAO Yang, JIAO Wei-yan, FAN Guang-hua, GAO Ya-chen

Citation:

HAN Jing, GAO Yang, JIAO Wei-yan, FAN Guang-hua, GAO Ya-chen. Mid-infrared plasmon regulation based on graphene nanoribbons[J]. *Chinese Optics*, 2020, 13(3): 627–636. doi: 10.3788/CO.2019–0185

韩晶, 高扬, 焦威严, 范光华, 高亚臣. 基于石墨烯纳米带的中红外等离子激元调控[J]. *中国光学*, 2020, 13(3): 627–636. doi: 10.3788/CO.2019–0185

View online: <https://doi.org/10.3788/CO.2019–0185>

---

### Articles you may be interested in

[Resonant mode of Fabry–Perot microcavity regulated by metal surface plasmons](#)

金属等离子激元调控Fabry–Perot微腔谐振模式研究

*Chinese Optics*. 2019, 12(3): 649 <https://doi.org/10.3788/CO.20191203.0649>

[Grating diffractive behavior of surface plasmon wave on meta–surface](#)

超表面上表面等离子激元波的光栅衍射行为研究

*Chinese Optics*. 2018, 11(1): 60 <https://doi.org/10.3788/CO.20181101.0060>

[Terahertz–wave devices based on plasmons in two–dimensional electron gas](#)

二维电子气等离子激元太赫兹波器件

*Chinese Optics*. 2017, 10(1): 51 <https://doi.org/10.3788/CO.20171001.0051>

[Optically controlled narrowband terahertz switcher based on graphene](#)

基于石墨烯的光学控制窄带太赫兹开关

*Chinese Optics*. 2018, 11(2): 166 <https://doi.org/10.3788/CO.20181102.0166>

[Multicolor fluorescent emission of graphene oxide and its application in fluorescence imaging](#)

氧化石墨烯的多色发光及其在荧光成像中的应用

*Chinese Optics*. 2018, 11(3): 377 <https://doi.org/10.3788/CO.20181103.0377>

[Recent progress in terahertz dynamic modulation based on graphene](#)

石墨烯太赫兹波动态调制的研究进展

*Chinese Optics*. 2017, 10(1): 86 <https://doi.org/10.3788/CO.20171001.0086>

## Mid-infrared plasmon regulation based on graphene nanoribbons

HAN Jing<sup>1,2</sup>, GAO Yang<sup>1</sup>, JIAO Wei-yan<sup>3</sup>, FAN Guang-hua<sup>3</sup>, GAO Ya-chen<sup>1\*</sup>

(1. College of Electronic Engineering, Heilongjiang University, Harbin 150080, China;

2. College of Science, Heilongjiang Institute of Technology, Harbin 150050, China;

3. College of Physics, Harbin Institute of Technology, Harbin 150001, China)

\* Corresponding author, E-mail: gaoyachen@hlju.edu.cn

**Abstract:** Surface plasmon can be produced in graphene in the mid-infrared and terahertz waveband regimes, and the regulation for surface plasmon can be achieved by a reasonable design. On the basis of above, a resonant tunable structure was designed. By depositing single layers of graphene ribbons with different widths on a dielectric substrate, discontinuities in nanoscale were introduced, thereby effectively controlling the interaction of graphene with light. The spectral and electromagnetic field distributions of the structure were theoretically studied using the finite difference time domain method. The results showed that when the designed structure was coupled with the incident light, there would be multiple resonance enhanced absorption peaks. By changing the number, width and distance of the graphene ribbons in each period, the number, position, intensity of the resonance peak can be controlled. In addition, the Fermi energy level of graphene can be changed by applying different bias voltages, so the position and intensity of resonance peak can be adjusted dynamically. Therefore, with this structure graphene plasmon resonance can be regulated over a wide spectral range. This study provides a theoretical basis for the design of the graphene-based sensors, filters and absorbers in infrared regime.

**Key words:** graphene ribbons; surface plasmon; Finite Difference Time Domain (FDTD); Fabry-Perot model; Fermi level

## 基于石墨烯纳米带的中红外等离子激元调控

韩晶<sup>1,2</sup>, 高扬<sup>1</sup>, 焦威严<sup>3</sup>, 范光华<sup>3</sup>, 高亚臣<sup>1\*</sup>

(1. 黑龙江大学电子工程学院, 黑龙江哈尔滨 150080;

2. 黑龙江工程学院理学院, 黑龙江哈尔滨 150050;

3. 哈尔滨工业大学物理学院, 黑龙江哈尔滨 150001)

**摘要:** 石墨烯在中红外和太赫兹波段可以产生表面等离子激元, 并且通过合理设计还可以对其表面等离子激元进行调控。基

收稿日期: 2019-09-17; 修订日期: 2019-10-21

基金项目: 黑龙江省自然科学基金(No. F2018027, No. LH2019F047)

Supported by Natural Scientific Foundation of Heilongjiang Province (No. F2018027, No. LH2019F047)

于此,本文设计了一种共振可调结构。通过在电介质基底上沉积不同宽度的单层石墨烯条带,引入纳米尺度上的不连续性,从而有效控制石墨烯与光的相互作用。使用时域有限差分法对该结构的光谱和电磁场分布进行了理论研究。结果表明:当所设计的结构与入射光耦合时,会出现多个共振增强的吸收峰;改变每个周期内石墨烯条带的数目、带宽和带间距,可以控制共振峰的个数、位置和强度;另外,施加不同的偏置电压可以改变石墨烯带的费米能级,从而实现共振峰位置和强度的动态调控;该结构可以在较宽光谱范围内调控石墨烯等离子激元。本文研究为设计中红外波段基于石墨烯的传感、滤波、吸收等器件提供了理论基础。

关键词:石墨烯条带;表面等离子激元;时域有限差分;法布里-珀罗模型;费米能级

中图分类号:TN29

文献标志码:A

doi:10.3788/CO.2019-0185

## 1 Introduction

The surface plasmon produced by precious metals such as gold and silver usually occurs in visible and near-infrared bands. However, in lower frequency bands, such as mid-infrared and terahertz bands, metals behave more like good conductors<sup>[1]</sup>. Therefore, the penetration and high space limitation of electric field disappears. In this case, graphene, whose electron density is much lower than that of precious metals, becomes an ideal substitute for generating the surface plasmons in the mid-infrared and terahertz bands. Graphene is a two-dimensional nanomaterial consisting of the hexagonal lattices of carbon atoms. With ultra-high carrier mobility, it can produce highly restricted surface plasmons in the mid-infrared and terahertz bands<sup>[2-3]</sup>. It can be mixed with other materials into high-performance composites<sup>[4]</sup> or integrated with the materials such as silicon<sup>[5]</sup>. It can also use external grid or chemical doping to dynamically control the carrier concentration<sup>[6-8]</sup>. Therefore, graphene is expected to be widely used in various functional devices such as photodetectors<sup>[9]</sup>, filters<sup>[10]</sup>, polarizers<sup>[11]</sup>, beam splitters<sup>[12]</sup> and tunable absorbers<sup>[13]</sup>.

However, graphene is only of atomic-level thickness. Its plasmon wave vector cannot effectively match the light wave vector in the infrared and terahertz bands in free space<sup>[14]</sup>, so the plasmon resonance in single-layer graphene is relatively weak. By patterning graphene into optical resonance nano-

structures (nanoribbons, nanodisks and so on)<sup>[15-17]</sup>, increasing the number of graphene layers<sup>[18]</sup> and coupling graphene with dielectric grating or resonator<sup>[19-21]</sup>, the plasmon resonance in graphene can be enhanced.

In this paper, a simple structure is proposed, in which the graphene nanoribbons of different widths are deposited on the infrared transparent substrate and then assembled into a ribbon array in parallel arrangement according to a certain periodic sequence. When light is incident on the structure, surface plasmon resonance is generated at the interface between the dielectric and the graphene. The surface plasmon polaritons propagating in the direction perpendicular to the ribbons are reflected back from the edge of the graphene, and then interfere with the light propagating forward, thus enhancing the graphene-light coupling. In this paper, the transmission, reflection and absorption spectra as well as electromagnetic field distribution of this structure are numerically studied by FDTD method. The results show that the absorption intensity of the proposed structure is increased. Moreover, by adjusting the number, width and spacing of graphene ribbons within a period, the number, position and intensity of resonance peaks can be regulated. In addition, by changing the bias voltage to adjust the Fermi level of graphene, the conductivity of graphene can be changed, so that the resonance can be adjusted conveniently, realizing the regulation for the plasmon resonance in a wider spectral range.

## 2 Structural model and primary theory

Figure 1 is schematic diagram of the proposed model within one period. The graphene is cut into two ribbons with a specific width ( $w_1$ ,  $w_2$ ), which is much smaller than the wavelength of the incident light. The ribbons are deposited on the substrate made of an infrared transparent material with the assumed refractive index of 1.4. A substrate is necessary for practical applications. It mainly affects the carrier mobility but does not change the basic scattering properties of graphene. The ribbons are periodically unrolled in the  $x$  direction ( $P = 2 \mu\text{m}$ ) and extended indefinitely in the  $y$  direction, with a distance of  $r$  between the ribbons. The light is incident along the negative  $z$ -axis and perpendicular to the structure, and the electric field is polarized along the  $x$ -axis. In the mid-infrared band, the conductivity of single-layer graphene can be described by Drude model<sup>[22]</sup>:

$$\sigma(\omega) = \frac{e^2 E_f}{\pi \hbar^2} \cdot \frac{i}{\omega + i\tau^{-1}}, \quad (1)$$

where  $\hbar$  is the reduced Planck constant,  $e$  is the electron charge,  $\omega$  is the resonant angular frequency,  $E_f$  is the Fermi level,  $\tau$  is the relaxation time ( $\tau = 1 \times 10^{-13}$  s). The Fermi level of graphene is  $E_f = 0.5$  eV.

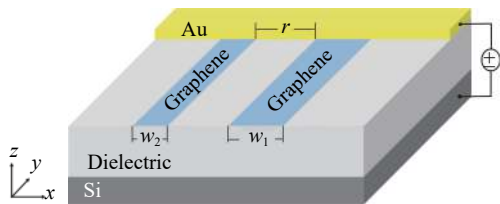


Fig. 1 Schematic diagram of graphene nanoribbon array with grid control within one period. The widths of the nanoribbons are  $w_1$  and  $w_2$ . The distance between the ribbons is  $r$

图1 具有栅极控制的石墨烯纳米条带阵列一个周期的示意图。纳米带的宽度分别为 $w_1$ ,  $w_2$ , 带间距离为 $r$

## 3 Results and discussion

The FDTD solutions is used to calculate the spectra of the structure. The Fig. 2 shows the transmission and reflection spectra of the proposed structure, including an illustration of absorption spectrum. In the Fig. 2,  $w_1 = 200$  nm,  $w_2 = 100$  nm,  $r = 100$  nm. As can be seen from Fig. 2, in the considered bands, there are three sharp transmission dips in the transmission spectrum of the structure. Accordingly, there are three narrow absorption peaks in the absorption spectrum, with a maximum absorption rate of 40%. The absorption rate is increased by an order of magnitude compared with uncut single-layer graphene<sup>[23]</sup>. The three resonance peaks are located at  $\lambda_1 = 11.92 \mu\text{m}$ ,  $\lambda_2 = 8.51 \mu\text{m}$ , and  $\lambda_3 = 6.25 \mu\text{m}$ , respectively.

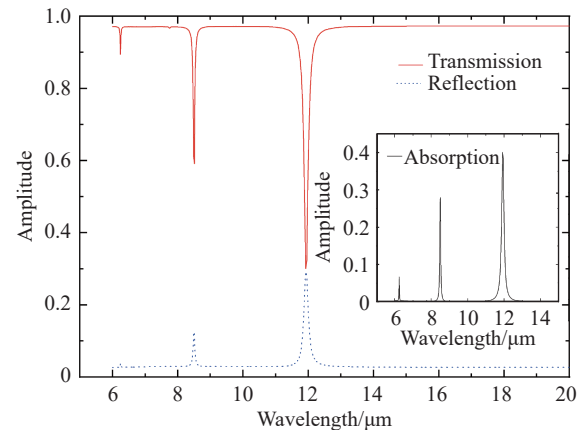


Fig. 2 Transmission, reflection and absorption (illustration) spectra of graphene nanoribbon structure. The widths of the nanoribbons are  $w_1 = 200$  nm and  $w_2 = 100$  nm, respectively. The distance between the nanoribbons is  $r = 100$  nm

图2 石墨烯纳米带结构的透射、反射、吸收(插图)光谱。纳米带宽度 $w_1 = 200$  nm,  $w_2 = 100$  nm, 带间距离 $r = 100$  nm

To clarify the mechanism of resonance formation, the Fig.3(a), Fig.3(b) and Fig.3(c) show the electric field distribution  $E_z$  in the  $z$  direction during resonance. It can be seen that when the resonance occurs, the electric fields on the upper and lower sides of the graphene ribbon edge as well as the

phases on both ends of the ribbon are in opposite directions. It can also be seen that the resonance caused by each graphene ribbon is independent. We can use the Fabry-Perot Model (F-P) to explain the above phenomenon. The dispersion relationship of graphene surface plasmons satisfies<sup>[20]</sup>:

$$\frac{\varepsilon_1}{\sqrt{k_{\text{GSP}}^2 - \varepsilon_1 k_0^2}} + \frac{\varepsilon_2}{\sqrt{k_{\text{GSP}}^2 - \varepsilon_2 k_0^2}} = -\frac{i\sigma}{\omega\varepsilon_0}, \quad (2)$$

where  $k_0 = \frac{\omega}{c}$  is the wave vector in the vacuum,  $c$  is the speed of light in the vacuum,  $k_{\text{GSP}}$  is the wave vector of graphene surface plasmon polaritons,  $\varepsilon_0$  is the dielectric constant in the vacuum,  $\varepsilon_1$  and  $\varepsilon_2$  are the relative dielectric constants of the dielectric on

both sides of the graphene,  $\sigma$  is the conductivity of the graphene surface. When the vertically incident light hits the edge of the graphene, it can produce the surface plasmon polaritons. When it is propagated to the other edge of the graphene, it will be reflected with a phase shift. When it is propagated forward, it will self-interfere with the surface plasmon polaritons that are reflected back. When satisfying

$$\Delta\varphi + R_r(k_{\text{GSP}})w = m\pi, \quad (3)$$

the interference will become stronger. In the equation,  $\Delta\varphi$  is the phase shift caused by reflection,  $w$  is the width of the graphene nanoribbons,  $m$  is the resonance order.

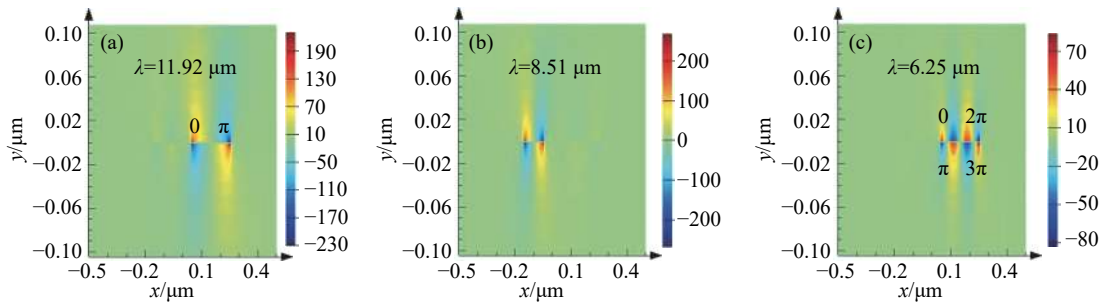


Fig. 3 Distributions of the electric field intensity  $E_z$  in  $z$  direction at different resonance wavelengths. The wavelengths of incident light are 11.92, 8.51 and 6.25  $\mu\text{m}$  respectively

图 3 不同共振波长下,  $z$  方向电场强度  $E_z$  的分布图。入射光波长分别为 11.92, 8.51, 6.25  $\mu\text{m}$

By substituting equation (3) into equation (2), and then using  $k = \frac{2\pi}{\lambda}$ , the resonance wavelength can be obtained

$$\lambda = 2\pi c \sqrt{\frac{\varepsilon_0 \hbar^2 (\varepsilon_1 + \varepsilon_2)}{e^2 E_f}} \cdot \frac{w}{m - \Delta\varphi/\pi}. \quad (4)$$

As can be seen from Fig. 3, the phases at both ends of the same graphene ribbon are contrary to each other, so  $m$  is assumed to be an odd number<sup>[20]</sup>. The simulation results  $\lambda_1 = 11.92 \mu\text{m}$  and  $\lambda_2 = 8.51 \mu\text{m}$  correspond to the resonance of two graphene ribbons ( $w_1 = 200 \text{ nm}$ ,  $w_2 = 100 \text{ nm}$ ) at the resonance order of  $m = 1$ . The result  $\lambda_3 = 6.25 \mu\text{m}$  correspond to the resonance of the graphene ribbon ( $w_1 = 200 \text{ nm}$ ) at the resonance order of  $m = 3$ . The

scattering of plasmon polaritons at the edge of graphene ribbons has been studied<sup>[24-25]</sup>. In our study, when  $\Delta\varphi = 0.3\pi$  is assumed, the positions of the resonance peaks calculated from equation (4) are  $\lambda_1 = 11.96 \mu\text{m}$ ,  $\lambda_2 = 8.47 \mu\text{m}$  and  $\lambda_3 = 6.10 \mu\text{m}$  respectively. The simulation results are in good agreement with the theoretical calculation results.

Fig. 4 shows the transmission spectra of the structure when the distances ( $r$ ) between two graphene nanoribbons are 140, 100, 60 and 20 nm respectively. When the distance is reduced from 140 nm to 60 nm, the positions of transmission dips (corresponding to the formants) remain almost unchanged. This is because no conductive charges exist on the dielectric layer between graphene ribbons,

and the surface plasmon polaritons propagating to the graphene edge are attenuated soon to prevent the coupling between adjacent graphene ribbons, each of which, as a result, produces independent resonance. When the distance between the graphene ribbons is reduced to 20 nm, the transmission dips are red-shifted due to the enhanced coupling between the ribbons. Therefore, by adjusting the distance between the ribbons, the coupling strength of their electromagnetic fields can be regulated so as to control the peak positions. In addition, when the distance between the graphene nanoribbons exceeds 100 nm, the interaction between them is already very weak. Therefore, the electromagnetic field scattered by the structure can be regarded as a linear combination of the scattering contributions of all the ribbons, thus we can conveniently regulate the interaction between light and matter. Based on this principle, we can extend the above structure into multiple graphene nanoribbons, and deposit the graphene nanoribbons with the corresponding width according to the desired peak positions. For example, four graphene nanoribbons with the widths of 250 nm, 200 nm, 150 nm and 100 nm respectively and with a spacing of 100 nm are introduced into one period. Fig. 5(a) is side view of the structure, and Fig. 5(b) shows its transmission and reflection spectra. It can be seen that there are six resonance peaks between 6  $\mu\text{m}$  and 20  $\mu\text{m}$ .  $\lambda_1$ ,  $\lambda_2$ ,  $\lambda_3$  and  $\lambda_4$  correspond to the resonance peaks of four graphene ribbons with the widths of  $w_1 = 250$  nm,  $w_2 = 200$  nm,  $w_3 = 150$  nm and  $w_4 = 100$  nm respectively in case of  $m = 1$ .  $\lambda_5$  and  $\lambda_6$  correspond to the resonance peaks of two graphene ribbons with the widths of  $w_1 = 250$  nm and  $w_2 = 200$  nm respectively in case of  $m = 3$ . It can be seen that, by adjusting the number and width of graphene ribbons within one period, the number and position of the peaks can be easily controlled.

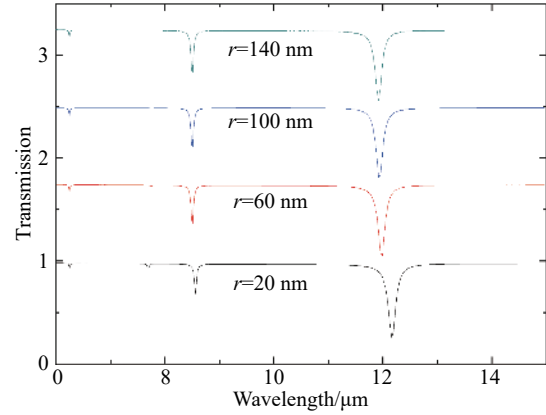


Fig. 4 Transmission spectra of the structure when the distance between graphene nanoribbons changes

图4 石墨烯纳米带间距变化时,结构的透射光谱

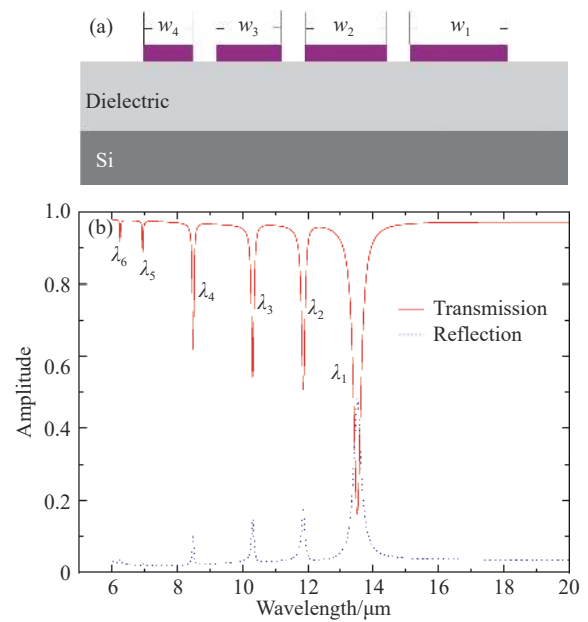


Fig. 5 (a) Side view of the structure. There are four graphene nanoribbons in one period. The widths of the nanoribbons are 250 nm, 200 nm, 150 nm and 100 nm respectively. (b) Transmission and reflection spectra of the structure

图5 (a) 为结构侧视图。一个周期内有4条石墨烯纳米带。条带宽度分别为250 nm, 200 nm, 150 nm, 100 nm。(b) 为该结构的透射谱、反射谱

In addition, effective dynamic adjustability of static electricity is a significant advantage of graphene plasmons<sup>[26-27]</sup>. By changing the bias voltage applied to the graphene ribbons to adjust the Fermi level, the concentration of graphene carriers can be controlled so that the peak positions can be

adjusted. Fig. 6 shows the resonance wavelength relative to the width of graphene ribbons at different Fermi levels ( $m = 1$ ,  $\Delta\varphi = 0.3\pi$ ). The curves are the

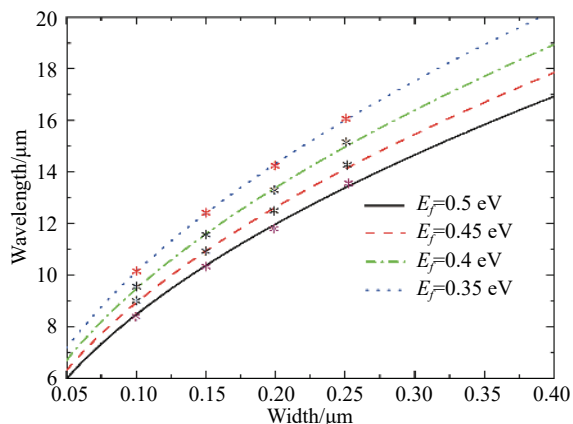


Fig. 6 Relationship between resonant wavelength and graphene ribbon width at different fermi levels

图 6 不同费米能级下,共振波长与石墨烯带宽度的关系

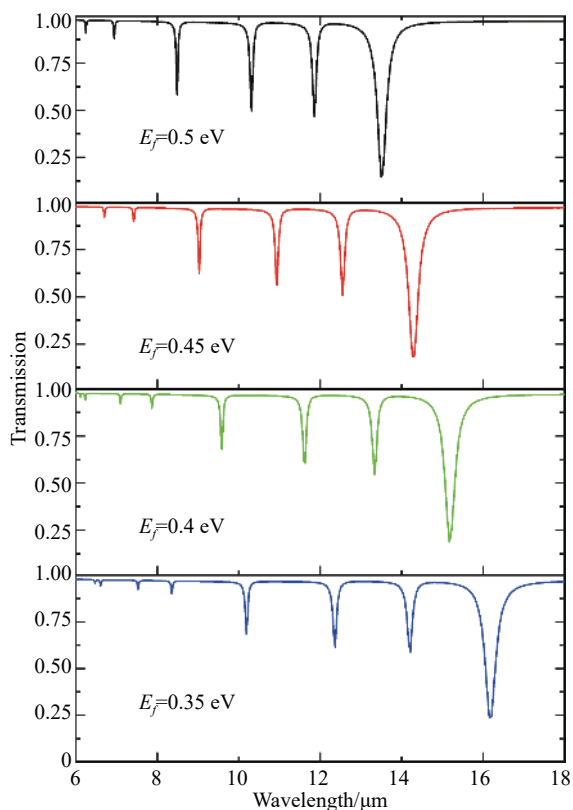


Fig. 7 Transmission spectra of structure with four graphene nanoribbons in a period at different Fermi levels

图 7 不同费米能级时,一个周期内 4 条石墨烯纳米带结构的透射光谱

theoretical calculation results obtained by equation (4), and the asterisks are the results of simulation calculation. There is good consistency between the two results.

Fig. 7 shows the transmission spectra of above structure with four graphene nanoribbons of different widths in a period at different Fermi levels. When  $E_f$  is changed from 0.5 eV into 0.35 eV, each resonance wavelength is obviously red-shifted. It can be seen from the figure that the structure has a strong capacity of electrostatic regulation. As long as the Fermi level is adjusted appropriately, the dynamic reversible regulation of resonance can be achieved in a wide spectral range.

## 4 Conclusion

In this paper, we designed a simple structure by cutting graphene into several nanoribbons and depositing them on a transparent infrared substrate to enhance the structure-light interaction. We used the Fabry-Perot model to explain the reason for resonance peak occurrence, and studied the influence the number, width and spacing of graphene nanoribbons on the number and position of peaks in one period. It was found that the electromagnetic wave was attenuated rapidly on the dielectric layer at the edge of the graphene nanoribbons. Therefore, when the distance between the nanoribbons exceeds a certain value, the coupling between the ribbons will become weak, and the light scattering by the structure can be regarded as a linear combination of the scattering effects of all the nanoribbons. In this way, the number and position of the occurring peaks can be controlled more flexibly and independently. In addition, by adjusting the Fermi level, the surface plasmons within graphene can be actively regulated in a wide spectral range. This study can contribute to the design of multifunctional and compact photonic devices based on simple graphene nanoribbon structures.

——中文对照版——

## 1 引言

利用金银等贵金属产生的表面等离子激元,通常处于可见光和近红外波段。在较低频率,例如中红外和太赫兹波段,金属表现得更像良导体<sup>[1]</sup>,此时,电场的穿透和高空间限制消失。而电子密度远低于贵金属的石墨烯成为在中红外和太赫兹波段产生表面等离子激元的理想替代品。石墨烯是一种由碳原子组成的具有六角晶格的二维纳米材料。它具有超高的载流子迁移率,在中红外和太赫兹波段可产生高度受限的表面等离子激元<sup>[2-3]</sup>,可以与其它材料形成性能优良的复合材料<sup>[4]</sup>或与硅等材料集成<sup>[5]</sup>,并且可以使用外部栅极或化学掺杂动态控制载流子浓度<sup>[6-8]</sup>。因此,石墨烯有望在光电探测器<sup>[9]</sup>,滤波器<sup>[10]</sup>,偏振器<sup>[11]</sup>,分束器<sup>[12]</sup>,可调谐吸收器<sup>[13]</sup>等各种功能器件中得到广泛应用。

但是石墨烯的厚度只有原子级,并且其中等离子激元波矢与红外和太赫兹波段自由空间中光波矢不能有效匹配<sup>[14]</sup>,使得单层石墨烯中等离子激元的共振相对较弱。通过将石墨烯图案化成光学共振纳米结构(纳米带或纳米盘等)<sup>[15-17]</sup>,增加石墨烯的层数<sup>[18]</sup>,与介质光栅或谐振腔耦合<sup>[19-21]</sup>等方法可以增强石墨烯中等离子激元共振。

本文提出一种简单的结构,在红外透明基底上沉积不同宽度的纳米石墨烯条带,再按一定周期平行排布组合成条带阵列。当光入射到该结构上时,在介质和石墨烯界面将产生表面等离子激元共振。沿垂直于条带方向传播的表面等离子激元传播到石墨烯边缘处反射回来,向前与反射回来的等离子激元发生干涉,从而增强了石墨烯与光的耦合作用。使用时域有限差分方法(FDTD)对该结构的透射、反射和吸收光谱以及电磁场分布进行了数值研究。该结构可使吸收强度有所提高。通过调节一个周期内石墨烯条带数目、宽度、间距,可以调控共振峰的数量、位置和强度。另外,通过改变偏置电压调整石墨烯的费米能级,可以改变石墨烯的电导率,从而方便地

对共振进行调节,实现了在较宽光谱范围内对等离子激元共振的调控。

## 2 结构模型和理论基础

图1是所提出的模型一个周期内的结构示意图,将石墨烯剪裁成两条特定宽度( $w_1, w_2$ )的条带,条带的宽度远小于入射光的波长,将条带沉积在基底上,选择一种红外透明材料做基底,设它的折射率为1.4。对于实际应用来说基底是必要的,它主要影响载流子的迁移率,但不会改变石墨烯的基本散射性质。条带是沿 $x$ 方向周期展开的,周期 $P = 2 \mu\text{m}$ ,沿 $y$ 方向无限延伸,条带之间的距离为 $r$ 。入射光沿着 $z$ 轴向下垂直入射到结构上,电场沿 $x$ 方向偏振。在中红外波段,单层石墨烯的电导率可以用Drude模型描述<sup>[22]</sup>:

$$\sigma(\omega) = \frac{e^2 E_f}{\pi \hbar^2} \cdot \frac{i}{\omega + i\tau^{-1}}, \quad (1)$$

其中 $\hbar$ 是约化普朗克常量, $e$ 是电子电量, $\omega$ 是共振角频率, $E_f$ 是费米能级, $\tau$ 是弛豫时间,取 $\tau = 1 \times 10^{-13} \text{ s}$ 。石墨烯的费米能级取 $E_f = 0.5 \text{ eV}$ 。

## 3 结果与讨论

利用FDTD Solutions时域有限差分软件计算结构的光谱。图2为所提出结构的透射、反射光谱,插图吸收光谱。其中 $w_1 = 200 \text{ nm}$ ,  $w_2 = 100 \text{ nm}$ ,  $r = 100 \text{ nm}$ 。从图中可以看出,在所考虑的波段内,结构的透射光谱出现了3个尖锐的透射谷,相应地吸收光谱出现了3个窄的吸收峰,吸收率最高达到40%,与未经裁剪的单层石墨烯相比,其吸收率提高了一个数量级<sup>[23]</sup>。3个共振峰分别位于 $\lambda_1 = 11.92 \mu\text{m}$ ,  $\lambda_2 = 8.51 \mu\text{m}$ ,  $\lambda_3 = 6.25 \mu\text{m}$ 。

为了明确共振形成的机理,图3(a)、3(b)、3(c)给出了共振时 $z$ 方向的电场分布 $E_z$ 。可以看出,共振时石墨烯带边缘上、下两侧电场方向相反,并且带两端的相位相反。也可以看出每个石墨烯带引起的共振是独立的。可以用法布里-珀

罗模型(F-P)解释上述现象。石墨烯表面等离激元的色散关系满足<sup>[20]</sup>:

$$\frac{\varepsilon_1}{\sqrt{k_{\text{GSP}}^2 - \varepsilon_1 k_0^2}} + \frac{\varepsilon_2}{\sqrt{k_{\text{GSP}}^2 - \varepsilon_2 k_0^2}} = -\frac{i\sigma}{\omega\varepsilon_0}, \quad (2)$$

其中:  $k_0 = \frac{\omega}{c}$ , 是真空中波矢,  $c$ 是真空中光速,  $k_{\text{GSP}}$ 是石墨烯表面等离极化激元波矢,  $\varepsilon_0$ 是真空中介电常数,  $\varepsilon_1, \varepsilon_2$ 分别是石墨烯两侧介质的相对介电常数,  $\sigma$ 是石墨烯表面的电导率。垂直入射的光照射到石墨烯边缘, 产生了表面等离极化激元, 当传播到石墨烯另一个边缘时, 会发生反射, 并产生了相移。向前传播与反射回来的表面等离极化激元将发生自干涉。当满足

$$\Delta\varphi + R_c(k_{\text{GSP}})w = m\pi \quad (3)$$

时, 干涉加强。其中 $\Delta\varphi$ 是反射产生的相移,  $w$ 是石墨烯纳米带的宽度,  $m$ 是共振级数。把式(3)代入式(2), 再利用 $k = \frac{2\pi}{\lambda}$ , 可以得到共振波长

$$\lambda = 2\pi c \sqrt{\frac{\varepsilon_0 \hbar^2 (\varepsilon_1 + \varepsilon_2)}{e^2 E_f}} \cdot \frac{w}{m - \Delta\varphi/\pi}. \quad (4)$$

由图3可知, 同一个石墨烯带两端的相位是相反的, 所以 $m$ 取奇数<sup>[20]</sup>。图3中,  $\lambda_1 = 11.92 \mu\text{m}$ ,  $\lambda_2 = 8.51 \mu\text{m}$ 为宽度 $w_1 = 200 \text{ nm}$ ,  $w_2 = 100 \text{ nm}$ 两个石墨烯带 $m = 1$ 时的共振波长,  $\lambda_3 = 6.25 \mu\text{m}$ 为宽度 $w_1 = 200 \text{ nm}$ 的石墨烯带 $m = 3$ 时的共振波长。已经有工作研究了等离极化激元在石墨烯带边缘的散射情况<sup>[24-25]</sup>。在本文的研究中, 当取 $\Delta\varphi = 0.3\pi$ 时, 由式(4)计算得出的共振峰的位置分别为 $\lambda'_1 = 11.96 \mu\text{m}$ ,  $\lambda'_2 = 8.47 \mu\text{m}$ ,  $\lambda'_3 = 6.10 \mu\text{m}$ , 仿真结果与理论计算得出的结果有良好的一致性。

图4为两个石墨烯纳米带距离 $r$ 分别为140 nm, 100 nm, 60 nm, 20 nm时结构的透射谱。可见, 距离由140 nm减少到60 nm时, 透射谷(对应于共振峰)的位置几乎不变。这是由于石墨烯带之间的介电层上不存在导电电荷, 表面等离极化激元传播到石墨烯边缘处很快衰退, 阻止了相邻石墨烯带间的耦合, 每个纳米带引起的共振是独立的。当石墨烯带间的距离减少到20 nm时, 透射谷出现了红移, 这是由于此时带之间的耦合作用增强。因此, 调整条带间距离可以调控它们之间

电磁场的耦合强度, 从而控制共振峰的位置。另外可以看到, 当石墨烯纳米带间距离超过100 nm时, 两个带之间的相互作用已经非常微弱了, 所以可将结构散射的电磁场看成是各条带散射贡献的线性组合, 这样为调控光与物质的相互作用增加了自由度。基于这种原理, 可以将上述的结构扩展成多条石墨烯纳米带, 根据想要获得的共振峰的位置沉积相应宽度的石墨烯带。例如在一个周期内引入4条石墨烯纳米带, 宽度分别为250, 200, 150, 100 nm, 间距为100 nm。图5(a)为该结构的侧视图。图5(b)为该结构的透射, 反射光谱。由图5可见, 在6  $\mu\text{m}$ 到20  $\mu\text{m}$ 之间出现了6个共振峰,  $\lambda_1, \lambda_2, \lambda_3, \lambda_4$ 分别对应于宽度为 $w_1 = 250 \text{ nm}$ ,  $w_2 = 200 \text{ nm}$ ,  $w_3 = 150 \text{ nm}$ ,  $w_4 = 100 \text{ nm}$ 的4个石墨烯带 $m = 1$ 时的共振峰。 $\lambda_5, \lambda_6$ 对应于宽度 $w_1 = 250 \text{ nm}$ ,  $w_2 = 200 \text{ nm}$ 的石墨烯带 $m = 3$ 时的共振峰。可见, 调整一个周期内石墨烯带的数量和宽度。可以方便地控制共振峰的数目和位置。

此外, 具有明显效果的静电动态可调特性是石墨烯等离激元的显著优点<sup>[26-27]</sup>。通过改变施加在石墨烯带上的偏置电压来调节费米能级, 控制石墨烯载流子浓度, 从而调节共振峰的位置。图6是不同费米能级时共振波长随石墨烯条带宽度变化的图像( $m = 1, \Delta\varphi = 0.3\pi$ ), 其中曲线是根据式(4)理论计算得出的结果, 星号是仿真计算结果, 可见, 二者有良好的一致性。图7显示了不同费米能级下, 上述一个周期内沉积4个不同宽度的石墨烯纳米带结构的透射光谱。可见,  $E_f$ 由0.5 eV变到0.35 eV时, 各个共振波长均发生明显红移。从图中可以看到, 该结构的静电调节能力很强, 只要适当地调整费米能级就可以在较宽的光谱范围内获得共振的动态可逆调节。

## 4 结 论

本文设计了一种简单的结构, 将石墨烯剪裁成纳米条带并沉积在红外透明基底上, 使得结构与光的相互作用增强。运用法布里-珀罗模型解释了共振峰出现的原因。研究了一个周期内石墨烯纳米带的数量、宽度和带间距的变化对共振峰

的影响。研究发现,电磁波在石墨烯纳米带边缘的介电层上快速地衰减,所以当纳米带之间的距离超过一定值时,带之间的耦合较弱,结构对光的散射可以看作各个纳米带散射效果的线性组合。这样就可以更灵活、独立地控制共振峰出现的数

量和位置,此外,调节费米能级还可以在较宽的光谱范围内主动调控石墨烯中的表面等离子体。这项研究有助于设计基于简单石墨烯纳米带结构的多功能和紧凑的光子学器件。

#### 参考文献:

- [1] YU N F, WANG Q J, KATS M A, *et al.*. Designer spoof surface plasmon structures collimate terahertz laser beams[J]. *Nature Materials*, 2010, 9(9): 730-735.
- [2] GEIM A K, NOVOSELOV K S. The rise of graphene[J]. *Nature Materials*, 2007, 6(3): 183-191.
- [3] GRIGORENKO A N, POLINI M, NOVOSELOV K S. Graphene plasmonics[J]. *Nature Photonics*, 2012, 6(11): 749-758.
- [4] LIU P W, JIN ZH, KATSUKIS G, *et al.*. Layered and scrolled nanocomposites with aligned semi-infinite graphene inclusions at the platelet limit[J]. *Science*, 2016, 353(6297): 364-367.
- [5] HAN S J, GARCIA A V, OIDA S, *et al.*. Graphene radio frequency receiver integrated circuit[J]. *Nature Communications*, 2014, 5: 3086.
- [6] REN L, ZHANG Q, YAO J, *et al.*. Terahertz and infrared spectroscopy of gated large-area graphene[J]. *Nano Letters*, 2012, 12(7): 3711-3715.
- [7] FEI Z, RODIN A S, ANDREEV G O, *et al.*. Gate-tuning of graphene plasmons revealed by infrared nano-imaging[J]. *Nature*, 2012, 487(7405): 82-85.
- [8] MIAO X CH, TONGAY S, PETERSON M K, *et al.*. High efficiency graphene solar cells by chemical doping[J]. *Nano Letters*, 2012, 12(6): 2745-2750.
- [9] CAI X H, SUSHKOV A B, JADIDI M M, *et al.*. Plasmon-enhanced terahertz photodetection in graphene[J]. *Nano Letters*, 2015, 15(7): 4295-4302.
- [10] GAO W L, SHU J, REICHEL K, *et al.*. High-contrast terahertz wave modulation by gated graphene enhanced by extraordinary transmission through ring apertures[J]. *Nano Letters*, 2014, 14(3): 1242-1248.
- [11] TAVAKOL M R, RAHMANI B, KHAVASI A. Tunable polarization converter based on one-dimensional graphene metasurfaces[J]. *Journal of the Optical Society of America B*, 2018, 35(10): 2574-2581.
- [12] TAVAKOL M R, SABA A, JAFARGHOLI A, *et al.*. Terahertz spectrum splitting by a graphene-covered array of rectangular grooves[J]. *Optics Letters*, 2017, 42(23): 4808-4811.
- [13] KIM S, JANG M S, BRAR V W, *et al.*. Electronically tunable extraordinary optical transmission in graphene plasmonic ribbons coupled to subwavelength metallic slit arrays[J]. *Nature Communications*, 2016, 7: 12323.
- [14] FARHAT M, GUENNEAU S, BAĞCI H. Exciting graphene surface plasmon polaritons through light and sound interplay[J]. *Physical Review Letters*, 2013, 111(23): 237404.
- [15] GARCIA-POMAR J L, NIKITIN A Y, MARTIN-MORENO L. Scattering of graphene plasmons by defects in the graphene sheet[J]. *ACS Nano*, 2013, 7(6): 4988-4994.
- [16] YAN H G, LI X S, CHANDRA B, *et al.*. Tunable infrared plasmonic devices using graphene/insulator stacks[J]. *Nature Nanotechnology*, 2012, 7(5): 330-334.
- [17] JIN ZH, SUN W, KE Y G, *et al.*. Metallized DNA nanolithography for encoding and transferring spatial information for graphene patterning[J]. *Nature Communications*, 2013, 4: 1663.
- [18] RODRIGO D, TITTL A, LIMAJ O, *et al.*. Double-layer graphene for enhanced tunable infrared plasmonics[J]. *Light: Science & Applications*, 2017, 6(6): e16277.
- [19] HUANG L, HU G H, DENG C Y, *et al.*. Realization of mid-infrared broadband absorption in monolayer graphene based on strong coupling between graphene nanoribbons and metal tapered grooves[J]. *Optics Express*, 2018, 26(22): 29192-29202.
- [20] ZHAO B, ZHANG ZH M. Strong plasmonic coupling between graphene ribbon array and metal gratings[J]. *ACS*

- Photonics*, 2015, 2(11): 1611-1618.
- [21] LI K, FITZGERALD J M, XIAO X F, *et al.*. Graphene plasmon cavities made with silicon carbide[J]. *ACS Omega*, 2017, 2(7): 3640-3646.
- [22] FALKOVSKY L A. Optical properties of graphene[J]. *Journal of Physics: Conference Series*, 2008, 129: 012004.
- [23] MAK K F, SFEIR M Y, WU Y, *et al.*. Measurement of the optical conductivity of graphene[J]. *Physical Review Letters*, 2008, 101(19): 196405.
- [24] DU L P, TANG D Y, YUAN X C. Edge-reflection phase directed plasmonic resonances on graphene nano-structures[J]. *Optics Express*, 2014, 22(19): 22689-22698.
- [25] CHEN J N, NESTEROV M L, NIKITIN A Y, *et al.*. Strong plasmon reflection at nanometer-size gaps in monolayer graphene on SiC[J]. *Nano Letters*, 2013, 13(12): 6210-6215.
- [26] LI Z Q, HENRIKSEN E A, JIANG Z, *et al.*. Dirac charge dynamics in graphene by infrared spectroscopy[J]. *Nature Physics*, 2008, 4(7): 532-535.
- [27] WANG F, ZHANG Y B, TIAN CH SH, *et al.*. Gate-variable optical transitions in graphene[J]. *Science*, 2008, 320(5873): 206-209.

#### 作者简介:



HAN Jing (1980—), female, born in Tianjin. She is a master and lecturer. She obtained her bachelor's degree and master's degree from Harbin Normal University in 2003 and 2006 respectively. She is mainly engaged in the research of micro-nano optics. E-mail: hanjing1980@163.com

韩晶(1980—),女,天津人,硕士,讲师,2003年、2006年于哈尔滨师范大学分别获得学士、硕士学位,主要从事微纳光学方面的研究。E-mail: hanjing1980@163.com



GAO Ya-chen (1969—), male, born in Chaoyang City, Liaoning Province. He is a doctor, professor and doctoral supervisor. He obtained his bachelor's degree from Liaoning Normal University in 1992, and his master's and doctor's degrees from Harbin Institute of Technology in 2001 and 2005 respectively. He is mainly engaged in the research of nonlinear optical materials, laser spectroscopy, nano-photonics and other fields. E-mail: gaoyachen@hlju.edu.cn

高亚臣(1969—),男,辽宁朝阳人,博士,教授,博士生导师,1992年于辽宁师范大学获得学士学位,2001年、2005年于哈尔滨工业大学分别获得硕士、博士学位,主要从事非线性光学材料、激光光谱学、纳米光子学等方面的研究。E-mail: gaoyachen@hlju.edu.cn